

## ANGULAR DEPENDENCE OF WAVE REFLECTION IN A LOSSY SINGLE-NEGATIVE BILAYER

**W.-H. Lin**

Department of Electrical Engineering  
Center for Micro/Nano Science and Technology  
Advance Optoelectronic Technology Center  
Institute of Microelectronics  
National Cheng-Kung University  
Tainan 70101, Taiwan

**C.-J. Wu**

Institute of Electro-Optical Science and Technology  
National Taiwan Normal University  
Taipei 11677, Taiwan

**S.-J. Chang**

Department of Electrical Engineering  
Center for Micro/Nano Science and Technology  
Advance Optoelectronic Technology Center  
Institute of Microelectronics  
National Cheng-Kung University  
Tainan 70101, Taiwan

**Abstract**—The angle-dependent properties of wave reflection in the lossy single-negative (SNG) materials are theoretically investigated. A model structure of SNG bilayer consisting of a lossy epsilon-negative (ENG) material and a lossy mu-negative (MNG) is considered in this work. The wave properties are investigated based on the calculated reflectance for the  $s$  wave (transversal electric wave) and the  $p$  wave (transversal magnetic wave) in addition to the degree of polarization. It is found that the angle-dependent reflectance of  $p$  wave is larger than that of  $s$  wave, which is contrary to the usual material with both positive epsilon and positive mu. The effects of losses coming from the

ENG and MNG materials are specifically explored and the roles played by their thicknesses are also numerically elucidated.

## 1. INTRODUCTION

With the existence of some novel and unique electromagnetic wave properties, electromagnetic metamaterials (MTMs) have recently attracted much attention [1–17]. In contrast to the conventional materials with their electromagnetic properties being derived from the microscopically atomic and molecular viewpoints, the electromagnetic material parameters of MTMs are effectively obtained based on the artificially manufactured structures. One of the familiar MTMs is called the double-negative (DNG) materials or left-handed materials (LHMs) because in this kind of material the electric field ( $\mathbf{E}$ ), the magnetic field ( $\mathbf{H}$ ) and the wave vector ( $\mathbf{k}$ ) form a left-handed triad. A DNG metamaterial was first theoretically studied earlier in 1968 by Veselago [18] and then was experimentally realized and demonstrated in 2000 by Smith et al. [19]. An important electromagnetic phenomenon that leads to many new modern applications is that of the so-called negative refraction (NR) or negative refractive index (NRI).

However, the terminology, NRI, with its definition has courted controversy from the inception of MTMs. The definition of NR or NRI has been clarified in a recent review paper by McCall [20]. In Ref. [20], the author pointed out that the definition should be extrinsic or intrinsic. The extrinsic definition involves an interface with another medium, whereas it is intrinsic to medium itself for the intrinsic definition. The intrinsic definition is based on criterion of the negative phase velocity (NPV), i.e., the phase velocity is antiparallel to the group velocity (or Poynting vector) The extrinsic one is related to the Snell's law of refraction. In fact, NRI is certainly meaningful for two-dimensional or three-dimensional structures. It is also advantageous to use these structures to emphasize the effectively homogeneous nature of LHMs. In one-dimensional structure, NRI, however, will lose its sense because the propagation angles may not be involved [21]. All these basic physics of negative refraction are well described and discussed in Ref. [20]. In this work, we just use the term DNG for interpreting the negative permittivity and negative permeability of a medium.

In order to satisfy the causality principle together with the Kramers-Kronig relations, a DNG material should be modeled as a dispersive and lossy medium [22]. The permittivity and permeability are thus both complex-valued, i.e.,  $\varepsilon = \varepsilon' + i\varepsilon''$  and  $\mu = \mu' + i\mu''$ . A DNG material is defined that its real parts of the permittivity and the permeability are both negative ( $\varepsilon' < 0$ ,  $\mu' < 0$ ) which in turn

lead to the negative refractive index, a fundamental and important consequence in a DNG metamaterial.

In addition to the DNG materials, there is other metamaterial called the single-negative (SNG) material of which only one of  $\varepsilon'$  or  $\mu'$  is negative. An SNG material can be classified as two types called the epsilon-negative (ENG) and mu-negative (MNG) as well. For a material with  $\varepsilon' < 0$  but  $\mu' > 0$  is referred to as an ENG material. An MNG material however is defined to has  $\mu' < 0$  but  $\varepsilon' > 0$ . In an SNG medium, it is seen that the refractive index (or wave number) is purely imaginary. Thus an electromagnetic wave will be totally reflected when it impinges on a single SNG slab because the wave is evanescent. However, the transmission can be highly enhanced by pairing the ENG and MNG media as an SNG bilayer structure [3, 5, 23]. In a lossless ENG-MNG bilayer, resonant tunneling can happen under the condition of impedance matching which can be well understood with the help of the transmission line model [23]. The tunneling feature in an SNG bilayer can be used to design the compact optical communication devices in a reduced length of system.

Using the lossless ENG-MNG bilayer as a unit cell in a one-dimensional SNG photonic crystal (PC), it is found that SNG photonic gap is quite different from that of the Bragg gap in a usual PC made of all double-positive (DPS) media. Such a new SNG gap is called the zero-effective-phase gap which originates from the interaction of forward and backward evanescent waves in SNG layers, a totally different mechanism from the Bragg gap. An SNG gap is omnidirectional and insensitive to the angle of incidence and the polarizations of light. In addition, it also is invariant with the change of length scale and even insensitive to the disorder [24, 25].

However, as mentioned previously, metamaterials are not only dispersive but lossy. The loss issue on the electromagnetic wave propagation in a lossy DNG slab was studied by Sabah and Uckun [26]. In a PC containing DNG materials, it has been shown that the losses strongly affect the photonic band structure [7, 27]. As for the SNG PCs, the SNG gaps are also influenced by incorporating the losses from the ENG and MNG materials [24, 28]. On the other hand, investigation of the loss issue on the wave propagation in a simple model structure of ENG-MNG bilayer is fundamentally important. Until recently, a study of loss effect on the wave propagation characteristics in this bilayer is reported [5]. It is shown that, in the normal incidence, a bilayer structure can enhance the transmission even when the loss increases. In addition, there exists a critical thickness of MNG layer such that the transmission through ENG-MNG bilayer attains a maximum. These two salient features are never seen in a lossy dielectric. As a result,

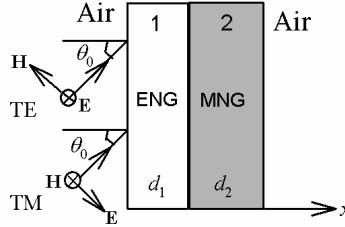


**Figure 1.** The structure of an SNG bilayer made of ENG and MNG materials. The thicknesses are ENG and MNG layers are  $d_1$  and  $d_2$ , respectively.

the lossy metamaterials can be used to improve the transmission in a simple layered structure.

The purpose of this paper is to extend the work of Ref. [5] to give a more complete analysis on the reflection properties in the general case of oblique incidence in a lossy ENG-MNG bilayer. The electromagnetic wave reflection as functions of the incidence angle, the polarization ( $s$  wave or  $p$  wave), and the losses from the ENG and MNG layers will be investigated through the calculated reflectance and the degree of polarization as well. The effects of thicknesses of the constituent layers are also given. It will be seen that the wave reflection in such a lossy bilayer has some unusual features that are fairly distinct to the usual lossy materials. The analysis gives some basic and useful information for the polarizing devices that are made of the SNG materials.

## 2. BASIC EQUATIONS

The SNG bilayer structure embedded in air ( $n_0 = 1$ ) is depicted in Fig. 1, where layers 1 and 2 are taken to be the ENG ( $0 < x < d_1$ ) and MNG ( $d_1 < x < d_1 + d_2$ ) materials, respectively. Assuming that the temporal part is  $\exp(-i\omega t)$  for all fields, the relative permittivity and relative permeability of an SNG material are described by the Drude model [5]. They are given by

$$\varepsilon_1 = \varepsilon'_1 + i\varepsilon''_1 = 1 - \frac{\omega_{ep}^2}{\omega^2 + i\omega\gamma_e}, \quad \mu_1 = a, \quad (1)$$

for an ENG material, and

$$\mu_2 = \mu'_2 + i\mu''_2 = 1 - \frac{\omega_{mp}^2}{\omega^2 + i\omega\gamma_m}, \quad \varepsilon_2 = b, \quad (2)$$

for an MNG material. Here  $\omega_{ep}$  and  $\omega_{mp}$  respectively denote the electric and magnetic plasma frequencies, and  $\gamma_e$  and  $\gamma_m$  are

the dissipation or loss coefficients of ENG and MNG, respectively. Hereafter, the dissipation coefficients,  $\gamma_e$  and  $\gamma_m$  will simply be referred to as the electric loss and magnetic loss, respectively. It can be seen from Eqs. (1) and (2) that there should exist some frequency range in order to obtain the negative real parts of  $\varepsilon_1$  and  $\mu_2$ . The frequency range depends on the values of the plasma and dissipation coefficient as well. Explicitly expressions for the real and imaginary parts of  $\varepsilon_1$  and  $\mu_2$  can be written by

$$\varepsilon'_1 = 1 - \frac{\omega_{ep}^2}{\omega^2 + \gamma_e^2}, \quad \varepsilon''_1 = \frac{\omega_{ep}^2 \gamma_e}{\omega^3 + \omega \gamma_e^2}, \quad (3)$$

and,

$$\mu'_2 = 1 - \frac{\omega_{mp}^2}{\omega^2 + \gamma_m^2}, \quad \mu''_2 = \frac{\omega_{mp}^2 \gamma_m}{\omega^3 + \omega \gamma_m^2}. \quad (4)$$

The corresponding refractive indices of ENG and MNG layers are thus given by  $n_j = \sqrt{\varepsilon_j \mu_j}$ ,  $j = 1, 2$ . It can be seen that the refractive indices of both ENG and MNG layers must be complex-valued, indicating that an electromagnetic wave is prohibited to propagate in a bulk SNG because the wave is evanescent. However, electromagnetic wave can actually penetrate and propagate through an SNG bilayer paired by ENG and MNG layers [3, 5, 23].

Let us consider that the wave is obliquely incident on the plane boundary,  $x = 0$ , at an angle of incidence of  $\theta_0$ . In the oblique incidence, there are two polarizations for the incident wave, i.e., the  $s$  wave (or the transversal electric (TE) wave) and the  $p$  wave (or the transversal magnetic (TM) wave), as illustrated in Fig. 1. Using the generalized Airy formula, the reflection coefficient at  $x = 0$  for this two-layer structure can be expressed as [29]

$$r = \frac{r_{01} + r_{123} e^{i2\phi_1}}{1 + r_{01} r_{123} e^{i2\phi_1}}, \quad (5)$$

with

$$r_{123} = \frac{r_{12} + r_{23} e^{i2\phi_2}}{1 + r_{12} r_{23} e^{i2\phi_2}}, \quad (6)$$

where subscripts 0 and 3 denote the air regions before layer 1 (ENG) and behind layer 2 (MNG), respectively, and

$$\phi_1 = \frac{2\pi}{\lambda} n_1 d_1 \cos \theta_1, \quad \phi_2 = \frac{2\pi}{\lambda} n_2 d_2 \cos \theta_2, \quad (7)$$

and  $r_{01}$ ,  $r_{12}$ , and  $r_{23}$  are the Fresnel reflections coefficients at three interfaces  $x = 0$ ,  $d_1$ , and  $d_1 + d_2$ , respectively. Fresnel reflection

coefficients from medium  $i$  to medium  $j$  ( $i, j = 0, 1, 2$  and  $3$ ) are given by

$$r_{ij} = \frac{(\eta_j / \cos \theta_j) - (\eta_i / \cos \theta_i)}{(\eta_j / \cos \theta_j) + (\eta_i / \cos \theta_i)}, \quad (8)$$

for  $s$  wave, and

$$r_{ij} = \frac{\eta_j \cos \theta_j - \eta_i \cos \theta_i}{\eta_j \cos \theta_j + \eta_i \cos \theta_i}, \quad (9)$$

for  $p$  wave, respectively, where

$$\eta_j = \eta_0 \sqrt{\frac{\mu_j}{\varepsilon_j}}, \quad (10)$$

is the intrinsic impedance of medium  $j$ , where  $\mu_j$  and  $\varepsilon_j$  are respectively the relative permeability and permittivity and  $\eta_0 = 377 \Omega$  is the intrinsic impedance of free space. In addition,  $\theta_j$  is the ray angle of medium  $j$  and becomes the incident angle for  $j = 0$ . The physical meaning of Eq. (6) represents a reflection coefficient of the composite structure consisting of a layer 2 sandwiched between medium 1 and 3.

Substituting Eq. (6) into Eq. (5) with simple manipulation, a complete expression for the reflection coefficient in a two-layer structure can be obtained to be

$$r = \frac{r_{01} + r_{12} \exp(2i\phi_1) + r_{23} \exp[2i(\phi_1 + \phi_2)] + r_{01} r_{12} r_{23} \exp(2i\phi_2)}{1 + r_{01} r_{12} \exp(2i\phi_1) + r_{12} r_{23} \exp(2i\phi_2) + r_{01} r_{23} \exp[2i(\phi_1 + \phi_2)]}. \quad (11)$$

The reflectance  $R$  is then given by

$$R = |r|^2. \quad (12)$$

With the two different polarizations, we shall denote the reflectance  $R_s$  and  $R_p$  for  $s$  and  $p$  waves, respectively. The degree of polarization is then, as usual, defined by

$$P = \frac{R_s - R_p}{R_s + R_p}. \quad (13)$$

In the common lossless DPS materials, in  $p$  wave, the angle-dependent  $P$  attains a maximum value of one when the incident angle reaches the so-called Brewster angle. The polarizing properties of the structure can be well learnt through the study of angular dependence of reflectance together with the degree of polarization.

Before we present the numerical results, we mention another method of obtaining the reflection coefficient. In Ref. [23], the transmission line model (TLM) is used to develop the reflection coefficient for the bilayer structure. Using TLM, the effective surface impedance  $Z_{s,eff}$  at the incident plane boundary of  $x = 0$  can be

calculated by successively making use of the impedance transform technique. Then the reflection coefficient is given by

$$r = \frac{Z_{s,eff} - \eta_0}{Z_{s,eff} + \eta_0}, \quad (14)$$

where  $Z_{s,eff}$  is given by

$$Z_{s,eff} = \eta_1 \frac{Z_s(z = d_1) + \eta_1 \tanh(\gamma_1 d_1)}{\eta_1 + Z_s(z = d_1) \tanh(\gamma_1 d_1)}, \quad (15)$$

with

$$Z_s(z = d_1) = \eta_2 \frac{\eta_0 + \eta_2 \tanh(\gamma_2 d_2)}{\eta_2 + \eta_0 \tanh(\gamma_2 d_2)}, \quad (16)$$

where the propagation constants in ENG layer and MNG layer are defined by

$$\gamma_j = -ik_j = -i\frac{\omega}{c}n_j, \quad j = 1, 2. \quad (17)$$

Although these formulas are valid for the case of normal incidence, they can be extended to the oblique incidence by capitalizing on the transverse impedance concept [30]. For example, all impedances,  $\eta_j$  ( $j = 0, 1, 2$ ) in the right-hand sides of Eqs. (14)–(16) should be replaced by the transverse impedance,  $\eta_{j,T}$ , which is given by

$$\eta_{j,T} = \eta_j / \cos \theta_j, \quad (18)$$

for  $s$  wave, and

$$\eta_{j,T} = \eta_j \cos \theta_j, \quad (19)$$

for  $p$  wave, respectively. In addition, the propagation constant in Eq. (17) should be modified as a longitudinal component, i.e.,

$$\gamma_j = -ik_j \cos \theta_j = -i\frac{\omega}{c}n_j \cos \theta_j, \quad j = 1, 2, \quad (20)$$

where  $c$  is the speed of light in free space. And the reflection coefficient can again be obtained by Eq. (14).

### 3. NUMERICAL RESULTS AND DISCUSSION

Let us now present the numerical results. In what follows we shall investigate the reflection properties for the lossy SNG materials. The material parameters to be used in the following calculations include  $\omega_{ep} = 10$  GHz and  $\omega_{mp} = 10\sqrt{3}$  GHz [5]. The operating frequency is taken to be  $\omega = 2\pi \times 1$  GHz.

### 3.1. Single ENG Layer

First, we examine a simple case of single ENG slab. In this case, the reflection coefficient can be simply obtained from Eq. (5) by replacing  $r_{123}$  by  $r_{10}$ . The permeability in Eq. (1) is  $\mu_1 = a = 3$  and the thickness of ENG layer is  $d_1 = 15$  mm. In Fig. 2, we have plotted the angle-dependent reflectance and degree of polarization for three different electric losses of  $\gamma_e = 0$  (a),  $2\pi \times 0.4$  GHz (b), and  $2\pi \times 0.8$  GHz (c), respectively.

In the absence of loss,  $\gamma_e = 0$ , it can be seen from Fig. 2(a) that both  $R_p$  and  $R_s$  start with a value of  $\sim 0.36$  at normal incidence.  $R_p$  increases with the increase in the angle of incidence, whereas  $R_s$  varies just a little bit for angle less than  $60^\circ$  and then increases as a function of the incident angle. It is of interest to find that the overall  $R_p$  is greater than  $R_s$  (except at  $0^\circ$  and  $90^\circ$ ), which shows sharply contrast to the usual DPS lossy materials. In the usual DPS media, it is known that  $R_s > R_p$ , which also holds even in a DNG slab [26]. With this opposite behavior, the peak in  $P$  at the Brewster angle in a DPS material will become a dip in an SNG material, as illustrated in Fig. 2. The dip with a value of  $-0.2$  occurs at the angle of near  $64^\circ$  at which the difference between  $R_p$  and  $R_s$  is a maximum. This angle is thus referred to as an effective Brewster angle.

In the presence of loss, in Fig. 2(b) with  $\gamma_e = 2\pi \times 0.4$  GHz, and Fig. 2(c) with  $\gamma_e = 2\pi \times 0.8$  GHz, the overall behaviors in  $R_s$ ,  $R_p$ , and  $P$  are similar to that of the lossless case in Fig. 2(a). The inclusion of loss decreases the values in both  $R_s$  and  $R_p$ . At  $\gamma_e = 2\pi \times 0.8$  GHz, the starting value at  $0^\circ$  has been lowered down to 0.2. It can also be seen that the dip in  $P$  is more salient as the loss increases. In addition, the effective Brewster angle has been shifted to  $68^\circ$  in Fig. 2(b) and  $70^\circ$  in Fig. 2(c).

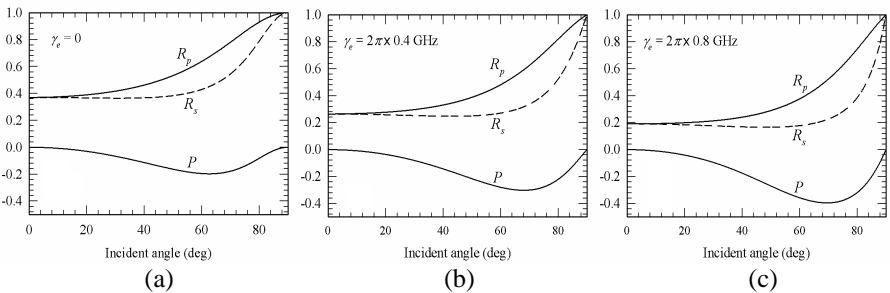


**Figure 2.** The angle-dependent reflectance  $R_s$  and  $R_p$ , and the degree of polarization  $P$  at three different losses in a single ENG layer.

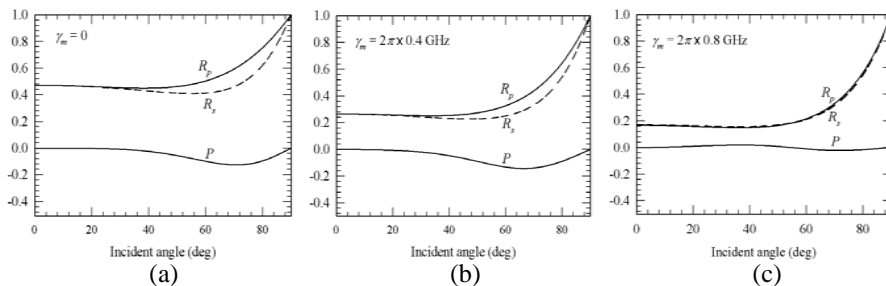


**Figure 3.** The angle-dependent reflectance  $R_s$  and  $R_p$ , and the degree of polarization  $P$  at three different magnetic losses in an ENG-MNG bilayer. Here the electric loss is fixed at  $\gamma_e = 2\pi \times 0.8$  GHz.

### 3.2. ENG-MNG Bilayer with Fixed $\gamma_e$

Let us now start to study the angular dependence of wave properties for an ENG-MNG bilayer. In this case, the permeability in Eq. (1) is  $\mu_1 = a = 1$  and the permittivity in Eq. (2) is  $\varepsilon_2 = b = 4$ . The thicknesses are taken to be  $d_1 = 10$  mm and  $d_2 = 40$  mm. In addition, we fix the electric loss at  $\gamma_e = 2\pi \times 0.8$  GHz and try to investigate how the magnetic loss influences the wave reflection. The angle-dependent reflection properties at three different magnetic losses of  $\gamma_m = 0$ ,  $2\pi \times 0.4$  GHz, and  $2\pi \times 0.8$  GHz are shown in Figs. 3(a), (b), and (c), respectively.

The reflection properties of the ENG-MNG bilayer shown in Fig. 3 are similar to that in Fig. 2 for a single ENG layer, that is,  $R_p > R_s$  is still seen. With a fixed electric loss  $\gamma_e$  of  $2\pi \times 0.8$  GHz in the ENG layer, the difference in  $R_s$  and  $R_p$  is reduced as the magnetic loss in the MNG layer increases. In Fig. 3(c), at a strong loss of  $\gamma_m = 2\pi \times 0.8$  GHz, the reflectance  $R_s$  and  $R_p$  nearly coincide, indicating that they are independent of the polarization of the incident wave. Thus, we conclude the polarization-dependent reflection properties will be nearly smeared out when both ENG and MNG are highly lossy.

### 3.3. ENG-MNG Bilayer with Fixed $\gamma_m$

If now the magnetic loss is kept at  $\gamma_m = 2\pi \times 0.8$  GHz and the electric loss  $\gamma_e$  is varied. The angle-dependent  $R_s$ ,  $R_p$ , and  $P$  at three different electric losses of  $\gamma_e = 0$ ,  $2\pi \times 0.4$  GHz, and  $2\pi \times 0.8$  GHz are shown in Figs. 4(a), (b), and (c), respectively. Comparing with Fig. 3, some features are of noted. First, Fig. 4(a) and Fig. 3(a) illustrate that the degree of polarization is more pronounced when  $\gamma_m = 2\pi \times 0.8$  GHz

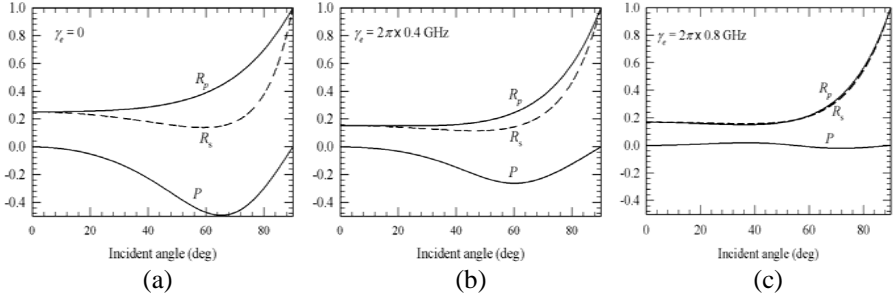


**Figure 4.** The angle-dependent reflectance  $R_s$  and  $R_p$ , and the degree of polarization  $P$  at three different electric losses in an ENG-MNG bilayer. Here the magnetic loss is fixed at  $\gamma_m = 2\pi \times 0.8$  GHz.

and  $\gamma_e = 0$ . Increasing the electric loss, as in Fig. 4(a) and Fig. 4(b), will reduce the magnitude of  $P$ , i.e., the difference between  $R_s$  and  $R_p$  is decreased.

### 3.4. ENG-MNG Bilayer under Different Thicknesses of $d_2$

Attention is now switched to the effects of film thickness. First, we explore how the thickness of the MNG layer affects the properties of reflection. We fix the thickness of ENG layer at  $d_1 = 10$  mm and both ENG and MNG are lossy, i.e., the electric loss and magnetic losses are taken to be equal to  $\gamma_e = \gamma_m = 2\pi \times 0.4$  GHz. The angle-dependent  $R_s$ ,  $R_p$ , and  $P$  at four MNG thicknesses,  $d_2 = 5, 10, 20,$  and  $40$  mm are plotted in Figs. 5(a), (b), (c) and (d), respectively.

It can be seen that the feature of  $R_p > R_s$  remains unchanged. At  $d_2 = 5$  mm (Fig. 5(a)), the variations in  $R_s$  and  $R_p$  are little and their values are negligibly small at angle less than  $60^\circ$ , indicating that there will be substantial transmission in this region even when they are lossy. Then  $R_s$  and  $R_p$  increase with increasing the angle. In addition, a large dip in  $P$  is obtained. Increasing  $d_2$  will enhance  $R_s$  and  $R_p$ , and make the dip in  $P$  shallow, as illustrated in Fig. 5(b) for  $d_2 = 10$  mm, Fig. 5(c) for  $d_2 = 20$  mm, and in Fig. 5(d) for  $40$  mm as well. The degree of polarization at four cases is depicted in Fig. 5(e). At  $d_2 = 5$  mm, the effective Brewster angle is  $53^\circ$ , where it is around  $66^\circ$  for the rest. A deep dip in  $P$  can be seen when  $d_2$  is small. For a thicker layer of  $d_2 > 20$  mm, the loss MNG layer will be large enough to treat as a open load. The reflection properties can thus be simply determined only by the first ENG layer according to the impedance transformation technique in the transmission lime model [23]. Therefore, the results

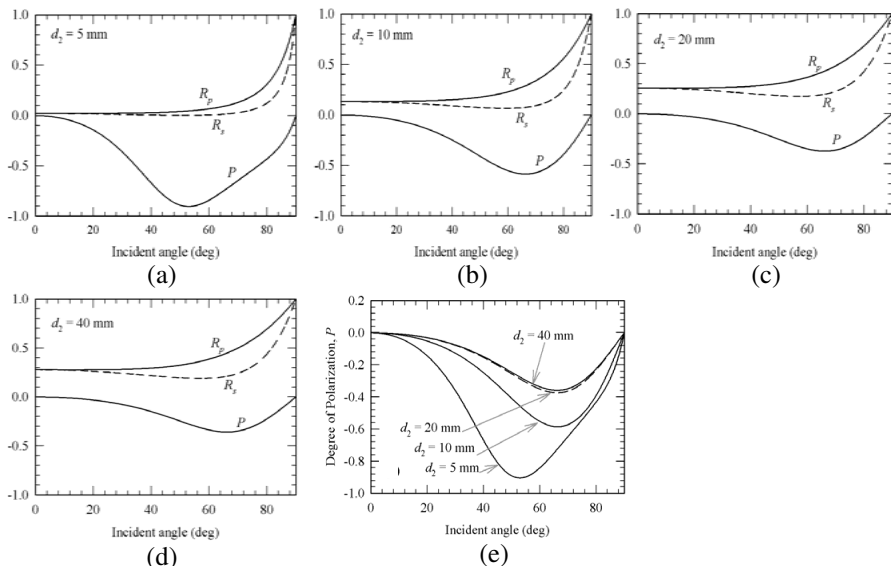


**Figure 5.** The angle-dependent reflectance  $R_s$  and  $R_p$ , and the degree of polarization  $P$  at four different  $d_2 = 5$  mm (a), 10 mm (b), 20 mm (c), and 40 mm (d) in an ENG-MNG bilayer. Here the electric and the magnetic loss are fixed at  $\gamma_m = 2\pi \times 0.4$  GHz. The four degrees of polarization are summarized in (e).

shown in Fig. 5(c) and Fig. 5(d) are quite analogous to that in Fig. 2(c) of a single ENG layer.

### 3.5. ENG-MNG Bilayer under Different Thicknesses of $d_1$

Finally, let us investigate the role played by  $d_1$ , the thickness of first ENG layer. For this, we fix the thickness of second MNG layer at  $d_2 = 15$  mm and both ENG and MNG are lossy with  $\gamma_e = \gamma_m = 2\pi \times 0.4$  GHz. The angle-dependent  $R_s$ ,  $R_p$ , and  $P$  at four ENG thicknesses,  $d_1 = 5, 10, 20,$  and  $40$  mm are plotted in Figs. 6(a), (b), (c) and (d), respectively. All the degrees of polarization are illustrated in Fig. 6(e).

Comparing Fig. 6 with Fig. 5, some salient features can be drawn. First, the feature of  $R_p > R_s$  remains unchanged for  $d_1 = 5$  mm (Fig. 6(a)), 10 mm (Fig. 6(b)), and 20 mm (Fig. 6(c)). The dip in  $P$  (Fig. 6(e)) is more pronounced as  $d_1$  increases, which is contrary to the role played by  $d_2$  in Fig. 5. Second, the magnitudes in  $R_p$  and  $R_s$

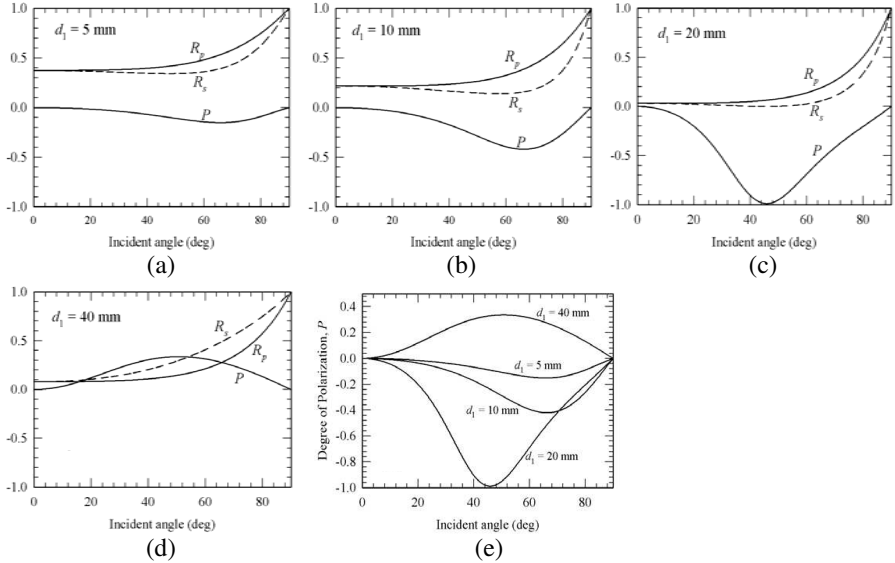


**Figure 6.** The angle-dependent reflectance  $R_s$  and  $R_p$ , and the degree of polarization  $P$  at four different  $d_1 = 5$  mm (a), 10 mm (b), 20 mm (c), and 40 mm (d) in an ENG-MNG bilayer. Here the electric and the magnetic loss are fixed at  $\gamma_m = 2\pi \times 0.4$  GHz. The four degrees of polarization are summarized in (e).

decrease as  $d_1$  increases, as depicted in Figs. 6(a), (b), and (c). This behavior is opposite to  $d_2$  in Fig. 5. Third, at a thicker ENG layer of  $d_1 = 40$  mm,  $R_p < R_s$ , behaving like a DPS or DNG material, and leading to the presence of a peak in  $P$  instead of a dip. This can be used to change the polarization of the reflected wave by changing the first ENG layer. Finally, in Fig. 6(e), the effective Brewster angles for these four cases are  $45.8^\circ$ ,  $66^\circ$ ,  $65.6^\circ$ , and  $50.4^\circ$ , respectively.

#### 4. CONCLUSION

Based on the calculated reflectance for the  $s$  and  $p$  waves together with the degree of polarization, the angular dependences of the reflection properties in the SNG materials have been systematically investigated. From the above analyses, some conclusions can be drawn and given as follows:

In a single ENG layer, it is found that  $R_p > R_s$ , in sharp contrast to lossy DPS and DNG materials. The angle-dependent  $R_s$  reveals the

unusual behavior with nearly independent of the incident angle being less than  $60^\circ$ .  $R_p$  is a sensitive function of the incident angle, increasing with increasing the angle. In addition, the degree of polarization can be enhanced when the electric loss increases.

In an ENG-MNG bilayer, the unusual result of  $R_p > R_s$  is still seen. In addition, the degree of polarization is increased by increasing the magnetic loss when the electric loss is fixed. Similar trend is also seen as the electric loss increases when the magnetic loss is fixed. Investigation of thickness effect reveals that thicker MNG layer will strongly decrease the value of degree of polarization as the thickness of ENG layer is fixed. However, a thicker ENG layer will enhance the degree of polarization when the thickness of MNG layer is fixed. Moreover, the dip shape in degree of polarization will eventually change to a peak at a much thicker ENG layer.

## ACKNOWLEDGMENT

C.-J. Wu acknowledges the financial support from the National Science Council of the Republic of China (Taiwan) under Contract No. NSC-97-2112-M-003-013-MY3.

## REFERENCES

1. Rahimi, H., A. Namdar, S. R. Entezar, and H. Tajalli, "Photonic transmission spectra in one-dimensional Fibonacci multilayer structures containing single-negative metamaterials," *Progress In Electromagnetics Research*, Vol. 102, 15–30, 2010.
2. Namdar, A., S. Roshan, H. Rahimi, and H. Tajalli, "Backward Tamm states in 1D single-negative metamaterials photonic crystals," *Progress In Electromagnetics Research Letters*, Vol. 13, 149–1159, 2010.
3. Ding, Y., Y. Li, H. Jiang, and H. Chen, "Electromagnetic tunneling in nonconjugated epsilon-negative and mu-negative metamaterials pair," *PIERS Online*, Vol. 6, No. 2, 109–112, 2010.
4. Hsu, H.-T. and C.-J. Wu, "Design rules for a Fabry-Perot narrow band transmission filter containing a metamaterial negative-index defect," *Progress In Electromagnetics Research Letters*, Vol. 9, 101–107, 2009.
5. Dong, L., G. Du, H. Jiang, H. Chen, and Y. Shi, "Transmission properties of lossy single-negative materials," *J. Opt. Soc. Am. B*, Vol. 26, 1091–1096, 2009.

6. Wang, Z.-Y., X.-M. Cheng, X.-Q. He, S.-L. Fan, and W.-Z. Yan, "Photonic crystal narrow filters with negative refractive index structural defects," *Progress In Electromagnetics Research*, Vol. 80, 421–430, 2008.
7. Canto, J. R., S. A. Matos, C. R. Paiva, and A. M. Barbosa, "Effects of losses in layered structure containing DPS and DNG media," *PIERS Online*, Vol. 4, No. 5, 546–550, 2008.
8. Chen, H. S., B. I. Wu, B. Zhang, and J. A. Kong, "Electromagnetic wave interactions with a metamaterial cloak," *Phys. Rev. Lett.*, Vol. 99, 063903-1–063903-4, 2007.
9. Cai, W., U. K. Chettiar, A. V. Kidishev, and V. M. Shalaev, "Optical cloaking with metamaterials," *Nature Photonics*, Vol. 1, 224–227, 2007.
10. Dolling, G., C. Enkrich, M. Wegener, C. M. Soukoulis, and S. Linden, "Simultaneous negative phase and group velocity of light in a metamaterial," *Science*, Vol. 312, 892–893, 2006.
11. Navarro-Cia, M., J. M. Carrasco, M. Beruete, and F. J. Falcone, "Ultra-wideband metamaterial filter based on electroinductive-wave coupling between microstrips," *Progress In Electromagnetics Research Letters*, Vol. 12, 141–150, 2009.
12. Wang, J., S. Qu, J. Zhang, H. Ma, Y. Yang, C. Gu, X. Wu, and Z. Xu, "A tunable left-handed metamaterial based on modified broadside-coupled split-ring resonators," *Progress In Electromagnetics Research Letters*, Vol. 6, 35–45, 2009.
13. Brovenko, A., P. N. Melezhib, A. Y. Poyedinchuk, N. P. Yashina, and G. Granet, "Resonant scattering of electromagnetic wave by stripe grating backed with a layer of metamaterial," *Progress In Electromagnetics Research B*, Vol. 15, 423–441, 2009.
14. Scher, A. D. and E. F. Kuester, "Boundary effects in the electromagnetic response of a metamaterial in the case of normal incidence," *Progress In Electromagnetics Research B*, Vol. 14, 341–381, 2009.
15. Ding, W., L. Chen, and C.-H. Liang, "Numerical study of goos-hänchen shift on the surface of anisotropic left-handed materials," *Progress In Electromagnetics Research B*, Vol. 2, 151–164, 2008.
16. Mirzavand, R., B. Honarbakhsh, A. Abdipour, and A. Tavakoli, "Metamaterial-based phase shifters for ultra wide-band applications," *Journal of Electromagnetic Waves and Applications*, Vol. 23, No. 11–12, 1489–1496, 2009.
17. Yu, G. X., T. J. Cui, W. X. Jiang, X. M. Yang, Q. Cheng, and Y. Hao, "Transformation of different kinds of electromagnetic

- waves using metamaterials,” *Journal of Electromagnetic Waves and Applications*, Vol. 23, No. 5–6, 583–592, 2009.
18. Veselago, V. G., “The electrodynamics of substances with simultaneously negative values of permittivity and permeability,” *Sov. Phys. Usp.*, Vol. 10, 509–514, 1968.
  19. Smith, D. R., W. J. Padilla, D. C. Vier, S. C. Nemat-Nasser, and S. Schultz, “Composite medium with simultaneous negative permeability and permittivity,” *Phys. Rev. Lett.*, Vol. 84, 4184–4187, 2000.
  20. McCall, M. W., “What is negative refraction?” *Journal of Modern Optics*, Vol. 56, 1727–1740, 2009.
  21. Caloz, C. and T. Itoh, *Electromagnetic Metamaterials: Transmission Line Theory and Microwave Applications*, John Wiley & Sons, NJ, 2006.
  22. Peiponen, K. E., V. Lucarini, E. M. Vartiainen, and J. J. Saarinen, “Kramers-Kronig relations and sum rules of negative refractive index medium,” *Eur. Phys. J. B*, Vol. 41, 61–65, 2004.
  23. Alu, A. and N. Engheta, “Pairing an epsilon-negative slab with a mu-negative slab: Resonance, tunneling and transparency,” *IEEE Trans. Antennas Propagation*, Vol. 51, 2558–2571, 2003.
  24. Wang, L. G., H. Chen, and S. Y. Zhou, “Omnidirectional gap and defect mode of one-dimensional photonic crystals with single-negative materials,” *Phys. Rev. B*, Vol. 70, 245102, 2004.
  25. Yeh, D.-W. and C.-J. Wu, “Analysis of photonic band structure in a one-dimensional photonic crystal containing single-negative material,” *Optics Express*, Vol. 17, 16666–16680, 2009.
  26. Sabah, C. and S. Uckun, “Electromagnetic wave propagation through frequency-dispersive and lossy double-negative slab,” *Opto-Electron. Rev.*, Vol. 15, 133–143, 2007.
  27. Hsu, H. T., K.-C. Ting, T.-J. Yang, and C.-J. Wu, “Investigation of photonic band gap in a one-dimensional lossy DNG/DPS photonic crystal,” *Solid State Comm.*, Vol. 150, 644–647, 2010.
  28. Yeh, D.-W. and C.-J. Wu, “Thickness-dependent photonic bandgap in a one-dimensional single-negative photonic crystal,” *J. Opt. Soc. Am. B*, Vol. 26, 1506–1510, 2009.
  29. Yeh, P., *Optical Waves in Layered Media*, John Wiley & Sons, Singapore, 1991.
  30. Orfanidis, S. J., *Electromagnetic Waves and Antennas*, Chapter 7, Rutgers University, 2008, [www.ece.rutgers.edu/~orfanidi/ewa](http://www.ece.rutgers.edu/~orfanidi/ewa).